Article

Palladium-Catalyzed Cross-Coupling Reaction via C–H Activation of Furanyl and Thiofuranyl Substrates

Neslihan Şahin [1,2,*], İsmail Özdemir [3] and David Sémeril [2,*]

1 Department of Science Education, Faculty of Education, Cumhuriyet University, Sivas 58040, Turkey
2 Synthèse Organométallique et Catalyse, UMR-CNRS 7177, Strasbourg University, 67008 Strasbourg, France
3 Department of Chemistry, Faculty of Science and Art, İnönü University, Malatya 44280, Turkey; ismail.ozdemir@inonu.edu.tr
* Correspondence: neslihan@cumhuriyet.edu.tr (N.Ş.); dsemeril@unistra.fr (D.S.); Tel.: +90-346-487-4656 (N.Ş.); +33-(0)3-6885-1550 (D.S.)

Abstract: The present study explores the potential of four NHC-palladium(II) complexes derived from (*Z*)- or (*E*)-styryl-*N*-alkylbenzimidazolium salts, namely *trans*-dichloro-[(*Z*)-1-styryl- 3-benzyl-benzimidazol-2-yliden]pyridine palladium(II) (**6**), *trans*-dichloro-[(*E*)-1-styryl-3-benzyl- benzimidazol-2-yliden]pyridine palladium(II) (**7**), *trans*-dichloro-[(*Z*)-1-styryl-3-(3-fluorobenzyl)- benzimidazol-2-yliden]pyridine palladium(II) (**8**) and *trans*-dichloro-[(*E*)-1-styryl-3- (3-fluorobenzyl)-benzimidazol-2-yliden]pyridine palladium(II) (**9**), to be use as pre-catalysts for the cross-coupling reactions between furanyl or thiofuranyl derivatives and arylbromides *via* the C–H activation of the heterocycles. The structures of the four Pd(II) complexes have been elucidated through the use of multinuclear NMR, FT-IR and mass spectroscopy. Furthermore, the *cis* or *trans* conformation of the styryl substituents and the geometry of two different compounds was substantiated by single-crystal X-ray diffraction, which was carried out on organometallic species **6**, **8** and **9**. After the optimization of catalytic conditions, which was carried out with 1 mol% of pre-catalyst with KOAc as a base in dimethylacetamide at 120 °C for 3 h, complex **6** proved to be the most effective pre-catalyst agent, with full or quasi full conversions being observed in the cross-coupling of 4-bromoacetophenone with 2-butylfuran, 1-(2-furanyl)-ethanone, furfuryl acetate, furfural, 1-(2-thienyl)-ethanone, thenaldehyde and 2-methylthiophene.

Keywords: palladium; benzimidazolium salt; styryl substituent; homogeneous catalysis; cross-coupling; C–H activation

1. Introduction

C–H bond activation has become an inescapable methodology for the formation of carbon–carbon bonds. Its success is mainly due to the fact that it is no longer necessary to use organic boron or metal reagents as in conventional cross-coupling reactions, which makes this reaction more economical and environmentally friendly [1–4].

To accomplish this greener carbon–carbon bond formation, several catalysts based on transition metals were developed. As an example, Oi, Inoue and co-workers arylated 2-arylpyridine at the ortho' position using 2.5 mol% of $[RuCl_2(\eta^6\text{-}C_6H_6)]_2$ and 10 mol% of triphenylphosphine (PPh_3). After 24 h at 120 °C in *N*-methylpyrrolidinone (NMP), the 2-(4-methyl-[1,1'-biphenyl]-2-yl)pyridine was isolated in a 95% yield from 2-(m-tolyl)pyridine and bromobenzene (Figure 1, Equation (1)) [5]. Bergman, Ellman and co-workers reported the rhodium-catalyzed arylation of heterocycles. When dihydroquinazoline and iodobenzene were reacted in THF over 6 h at 150 °C with $[RhCl(coe)_2]_2$ (coe = cyclooctene) and PCy_3 in the presence of Et_3N, the corresponding 2-phenylquinazoline was isolated in a 78% yield. In such catalytic conditions, the 2-phenyldihydroquinazoline intermediate underwent a dehydrogenation reaction. According to the authors, arylation is believed to proceed via an NHC intermediate (Figure 1, Equation (2)) [6].

Although many transition metals can be used, palladium-based complexes remain the most popular for C–H activation [7–11]. In this context, Fagnou and co-workers reported the intramolecular formation of biaryl compounds using the in situ-generated catalytic system made of [Pd(OAc)$_2$] and 2-(diphenylphosphino)-2′-(*N,N*-dimethyl- amino)biphenyl. Using a catalyst loading as low as 0.2 mol%, 98% of the tricyclic biaryl compound was isolated after 14 h at 145 °C in dimethylacetamide (DMAc) (Figure 1, Equation (3)) [12]. Many research groups have focused on coupling reactions between heteroarenes and aryl halides in the presence of a base, often in DMAc (Figure 1, Equation (4)). For example, the group of Aktaş used 0.3 mol% of the *N*-propylphthalimide-substituted [bis-(NHC)PdBr$_2$] complex (**A**; Figure 1) (NHC = *N*-heterocyclic carbene) as a pre-catalyst in the cross-coupling between 2-butylthiophene and 4-bromoacetophenone or 4-bromotoluene in DMAc using KOAc as a base after 1 h at 130 °C, and 94 and 99%, respectively, of the substrates were converted [13]. This aryl bromide has been used for the direct arylation of substituted 4-(thiophen-2-yl)pyridine by the group of Srinivasa using 1 mol% of [PdBr$_2$(NHC-)Py] from coumarin tethered NHC as a pre-catalyst (**B**; Figure 1). After 24 h at 80 °C, using K$_2$CO$_3$ as a base and PivOH as an additive, a product formed with 4-bromotoluene was obtained with a conversion of 94% [14].
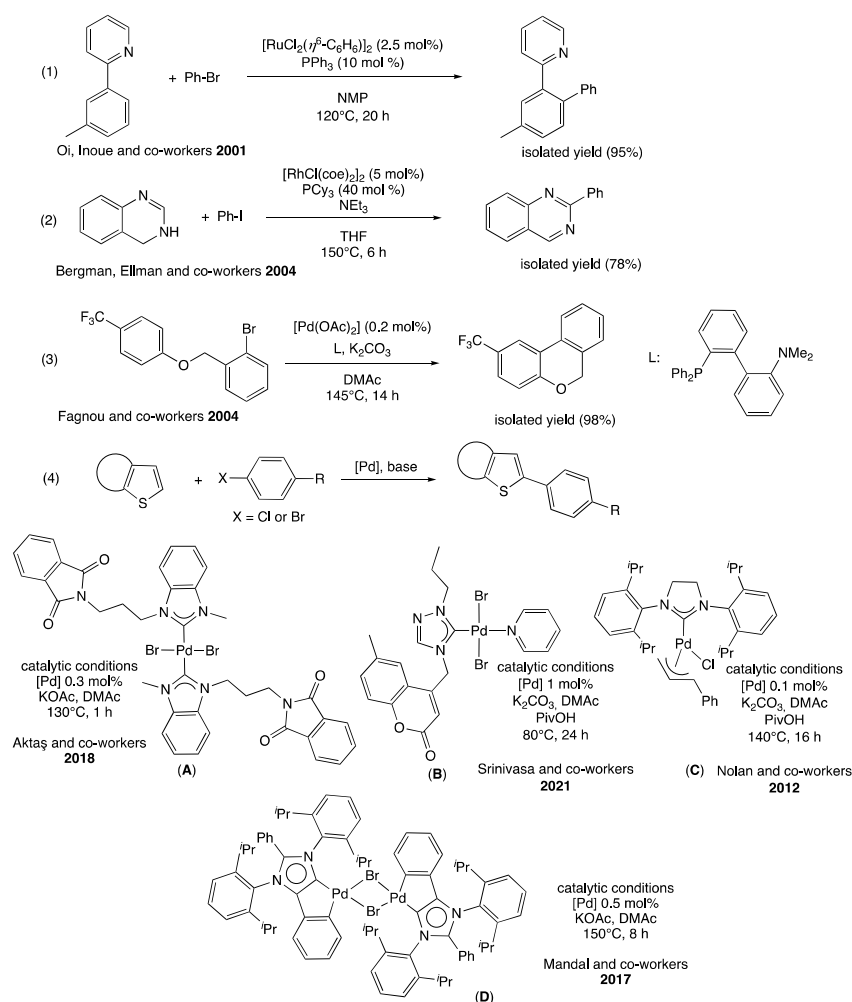

Figure 1. Selected examples of reported C–H activations for the formation of carbon–carbon bonds [5,6,12–16].

The direct arylation of benzothiophene was achieved, for example, with 4-bromotoluene or 4-bromoanisole with conversions of 89 and 70%, respectively, with a catalyst loading of only 0.1 mol%, using the [Pd(SIPr)(cinnamyl)Cl] complex (**C**; Figure 1) as a pre-catalyst with K$_2$CO$_3$ and PivOH over 16 h at 140 °C in DMAc [15]. Dimeric complex **D** (Figure 1),

consisting of two abnormal *N*-heterocyclic carbenes, is an effective coupling promoter for the cross-reaction between benzothiophene and the more challenging 4-chlorobenzonitrile (conversion of 41%). The group of Mandal carried out the catalytic test in DMAc using a catalyst loading of 0.5 mol% at 150 °C over 8 h [16].

Initially developed by the group of Organ [17], Pd-PEPPSI-NHC complexes (PEPPSI = Pyridine-Enhanced Pre-catalyst Preparation Stabilization and Initiation) [18,19], thanks to their easy decoordination of the ancillary ligand and the formation of the active Pd(0) species [20], have been shown to be particularly efficient in cross-coupling, such as the Suzuki–Miyaura [21–23], Mizoroki–Heck [23,24], Kumada–Tamao–Corriu [25], Negishi [26], Sonogashira [23,27], and Buchwald–Hartwig reactions [28,29] or the activation of the C–H bonds of heteroarenes [30–33].

In this context, and based on our experience of ligand design for the preparation of palladium of PEPPSI-type complexes [34] for the direct arylation of heteroarenes [35–43], we report the palladium-catalyzed C–H activation of furanyl and thiofuranyl substrates in which the *N*-heterocyclic carbenes incorporate, for the first time, (*E*)- or (*Z*)-styryl-benzimidazole moieties (Figure 2).
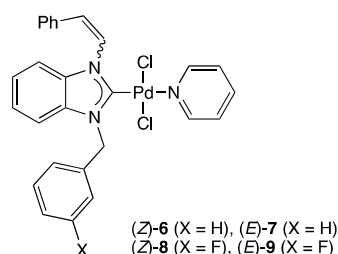

(*Z*)-**6** (X = H), (*E*)-**7** (X = H)
(*Z*)-**8** (X = F), (*E*)-**9** (X = F)

Figure 2. Targeted palladium pre-catalysts **6**–**9** based on (*E*)- or (*Z*)-styryl-benzimidazole moieties.

2. Results and Discussion

2.1. Synthesis of Palladium(II) Complexes

The synthesis of the four targeted Pd(II) complexes **6**–**9** required the preparation of adequate benzimidazolium salts **3**–**5**. These salts were obtained by the alkylation of (*E*)- or (*Z*)-styryl-benzimidazole **1** and **2**, respectively, with benzyl chloride or 3-fluorobenzyl chloride in DMF at 80 °C for 24 h (Scheme 1). After precipitated by the addition of Et$_2$O, the three salts were isolated in 59–73% yields and fully characterized by FT-IR, ^{1}H, ^{13}C and ^{19}F NMR spectroscopy and an elemental analysis (see the Experimental Procedure Section and Supplementary Materials). The ^{1}H NMR spectra of these compounds show a significant downfield of the NCHN proton, which appeared in the range from 10.12 to 11.49 ppm. It is interesting to note that the presence of a fluorine atom in position 3 of the aromatic cycle (salt **4**) has no influence on the σ-donor properties. Indeed, the careful study of the ^{1}H spectra of salts **3** (without a F atom) and **4** (with a F atom) revealed no difference between the two $^1J_{HC}$ constants (222.3 Hz). These values are close to that measured for the well-known 1,3-di(2,6-diisopropylphenyl)-imidazolium chloride (IPr.HCl) salt [44].

The two NHC-complexes bearing the benzyl substituents **6** and **7** were obtained from (*Z*)-1-styryl-3-benzyl-benzimidazolium chloride (**3**) through the reaction with [PdCl$_2$] in the presence of K$_2$CO$_3$ in pyridine (Scheme 2). It is important to mention that the temperature of the reaction determines the configuration of the double bond of the styryl substituent. When the reaction was carried out at 80 °C, the *cis* geometry of the double bond was maintained with coupling constants of $^3J_{HH}$ = 8.5 Hz for the two NCH=CHPh signals (complex **6**). Conversely, a reaction temperature of 120 °C resulted in the isomerization of the double bond, and the *trans* complex **7** was isolated in a 61% yield ($^3J_{HH}$ = 14.5 Hz for the NCH=CHPh signals).
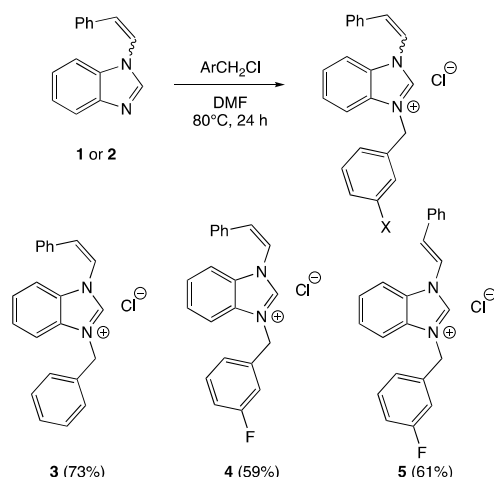
Scheme 1. Synthesis of styryl benzimidazolium salts **3**–**5**.
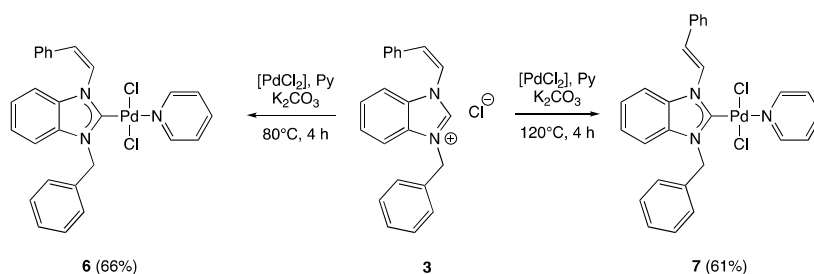
Scheme 2. Synthesis of Pd(II) (*Z*)-**6** and (*E*)-**7** complexes.

Taking this observation into account, fluorinated Pd(II) complexes **8** and **9** were prepared from salts **4** and **5**, respectively, with stoichiometric amounts of [PdCl$_2$] and K$_2$CO$_3$ in pyridine at 80 °C (Scheme 3). Both complexes were isolated in 65–67% yields and, according to their ^{1}H NMR spectra, no isomerization of the double bond was observed.
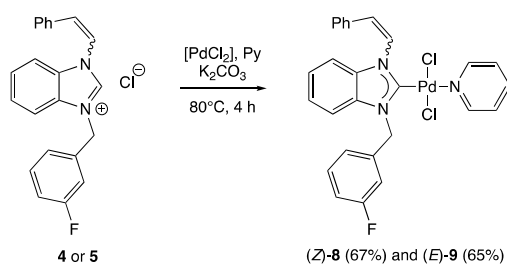
Scheme 3. Synthesis of fluorinated Pd(II) complexes **8** and **9**.

The four Pd(II) complexes were fully characterized by FT-IR, ^{1}H, ^{13}C and ^{19}F NMR spectroscopy, an elemental analysis and mass spectroscopy (see the Experimental Procedure Section and Supplementary Materials). The ^{1}H spectra showed the presence of the pyridine ligand coordinated to the metal center and the disappearance of the NCHN protons of the benzimidazole moieties. Moreover, the ^{13}C spectra displayed a downfield of the corresponding carbon atoms from 141.00 to 143.73 ppm in benzimidazolium salts **3**–**4** to 165.15–165.87 ppm in complexes **6**–**9**, which are characteristic of the formation of Pd-NHC bonds [28,32]. Finally, a mass spectra analysis revealed the presence of peaks corresponding to either [M − Cl]$^+$ or [M + H]$^+$ cations with the expected isotopic profiles.

2.2. X-ray Crystal Structure Analysis of Palladium(II) Complexes

Single crystals of Pd(II) complexes **6**, **8** and **9**, which were suitable for X-ray analysis, unambiguously confirmed the formation of the attempt complexes.

Complexes **6** (Figure 3) and **8** (Figure 4), due to the *cis* configuration of the styryl substituent blocking free rotation around the N-C bond, crystallized in the orthorhombic chiral Sohncke group P2$_1$2$_1$2$_1$ [45] with Flack parameters of 0.07(4) and −0.04(4), respectively [46]. In both solid-state structures, four molecules of complexes were present in the unit cell, and each Pd(II) atom adopted a square planar geometry with C1-Pd1-N3 angles of 176.5(3) and 176.7(2)° and Cl1-Pd1-Cl2 angles of 176.80(7) and 177.83(8)° in complexes **6** and **8**, respectively. The bond lengths of Pd-C1 were found to be 1.966(7) and 1.938(6) Å in complexes **6** and **8**, respectively, which are distances in agreement for Pd-NHC bonds [47]. The benzimidazole aromatic rings were almost planar with the pyridine moieties, with dihedral angles of 8.49 and 6.79°, in complexes **6** and **8**, respectively, and inclined relative to the phenyl of the styryl substituents with dihedral angles of 57.14 and 60.34° in complexes **6** and **8**, respectively.

Figure 3. ORTEP drawing of Pd(II) complex **6** with 50% probability of thermal ellipsoids. Important bond lengths (Å) and angles (°): Pd1-C1 1.966(7), Pd1-Cl1 2.313(2), Pd1-Cl2 2.318(2), Pd1-N3 2.095(6), C1-N1 1.363(9), C1-N2 1.354(9), C8-C9 1.334(11), C1-Pd1-Cl1 88.1(2), Cl1-Pd1-N3 89.56(18), N3-Pd1-Cl2 93.05(19), Cl2-Pd1-C1 89.4(2), C1-Pd1-N3 176.5(3) and Cl1-Pd1-Cl2 176.80(7).

Figure 4. ORTEP drawing of Pd(II) complex **8** with 50% probability of thermal ellipsoids. Important bond lengths (Å) and angles (°): Pd1-C1 1.938(6), Pd1-Cl1 2.3018(15), Pd1-Cl2 2.3056(15), Pd1-N3 2.083(6), C1-N1 1.354(8), C1-N2 1.372(8), C15-C16 1.307(9), C1-Pd1-Cl1 89.25(19), Cl1-Pd1-N3 89.59(17), N3-Pd1-Cl2 92.35(17), Cl2-Pd1-C1 88.87(19), C1-Pd1-N3 176.7(2) and Cl1-Pd1-Cl2 177.83(8).

Complex **9** (Figure 5) crystallized in the monoclinic form with the C2/c space group. Eight molecules of complexes were present in the unit cell. The fluorine atom was disordered over two positions with a ratio of 0.6/0.4. As previously mentioned, the Pd(II) atom adopted a square planar geometry with C1-Pd1-N3 and Cl1-Pd1-Cl2 angles of 179.82(17) and 177.78(6), respectively. The bond lengths of Pd-C1 and Pd-N3 were found to be 1.959(5) and 2.076(4) Å, respectively. In the present complex, the phenyl of the styryl substituent was slightly inclined to the benzimidazole and to the pyridine rings with dihedral angles of 14.76 and 10.91°, respectively.
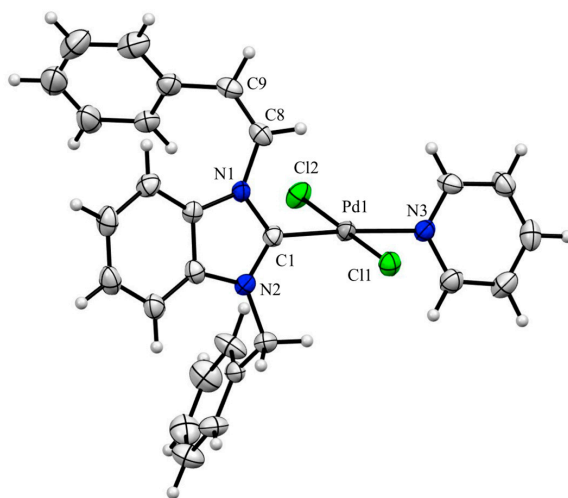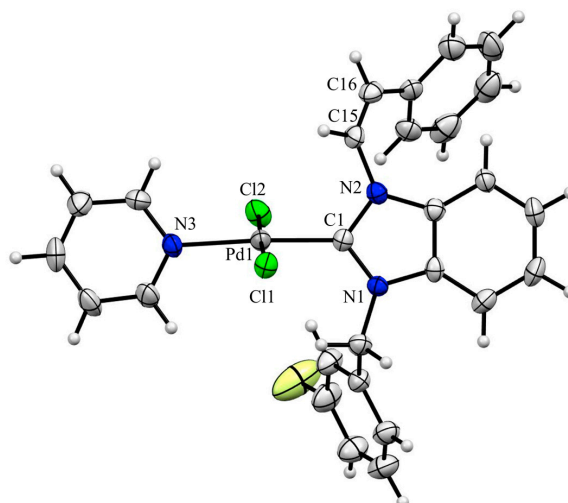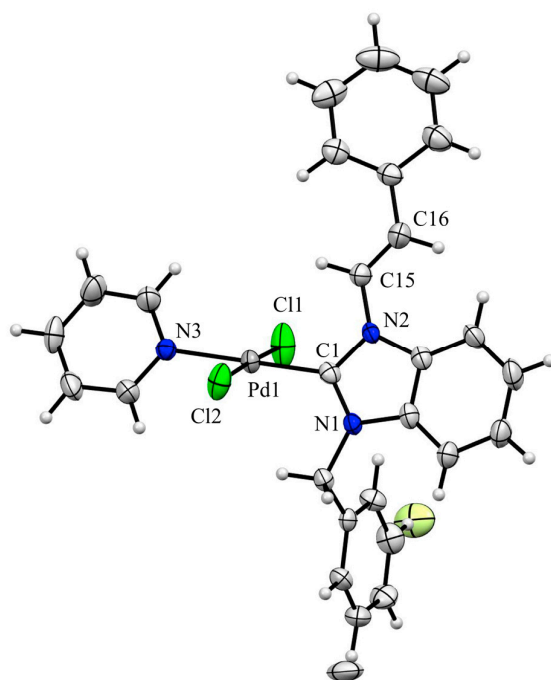

Figure 5. ORTEP drawing of Pd(II) complex **9** with 50% probability of thermal ellipsoids. Important bond lengths (Å) and angles (°): Pd1-C1 1.959(5), Pd1-Cl1 2.2820(14), Pd1-Cl2 2.2968(13), Pd1-N3 2.076(4), C1-N1 1.350(6), C1-N2 1.354(6), C15-C16 1.292(7), C1-Pd1-Cl1 89.36(13), Cl1-Pd1-N3 90.68(11), N3-Pd1-Cl2 90.56(11), Cl2-Pd1-C1 89.40(13), C1-Pd1-N3 179.82(17) and Cl1-Pd1-Cl2 177.78(6).
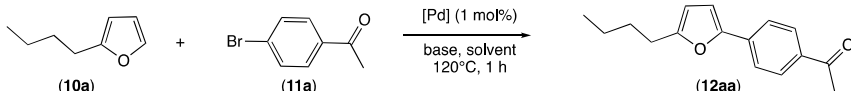
2.3. Palladium-Catalyzed C–H Activation

We tested the four PEPPSI-type Pd(II) complexes **6**–**9** in the C–H activation of furanyl and thiofuranyl substrates. In the initial phase, the optimal catalytic conditions were determined. For this, the cross-coupling reaction between 2-butylfuran (**10a**) and the 4-bromoacetophenone (**11a**) was tested with complex **6** as the pre-catalyst (Table 1).

In the first series of runs, six bases were tested in DMAc as a solvent at 120 °C for 1 h. When potassium hydroxide (KOH) and potassium *tert*-butoxide (*t*BuOK) were employed, no formation of the attempt 1-(4-(5-butylfuran-2-yl)phenyl)ethanone (**12aa**) was observed (Table 1, entries 1 and 2). Modest conversions were measured with alkali metal carbonates (Cs⁺: 15% and K⁺: 21%; Table 1, entries 3 and 4). In contrast, alkali metal acetates led to high conversions up to 76% when K⁺ was associated as a cation (Table 1, entries 5 and 6).

In the second series of runs, the solvent was evaluated. Changing DMAc with toluene or dimethylsulfoxide (DMSO) drastically decreased the conversions (Table 1, entries 7 and 8). A modest conversion of 54% was obtained when *N*,*N*-dimethylformamide (DMF) was employed (Table 1, entry 9).

The optimum found solvent (DMAc) and base (KOAc) are the same as those generally employed in this cross-coupling reaction [13,41–43].

Table 1. Palladium-catalyzed formation of 1-(4-(5-butylfuran-2-yl)phenyl)ethanone (**12aa**); search for optimal conditions: effect of base, solvent and palladium precursor [1].

Entry	Complex	Base	Solvent	Conversion (%) [2]
1	6	KOH	DMAc	/
2	6	^{t}BuOK	DMAc	/
3	6	Cs_2CO_3	DMAc	15
4	6	K_2CO_3	DMAc	21
5	6	NaOAc	DMAc	71
6	6	KOAc	DMAc	76
7	6	KOAc	Toluene	4
8	6	KOAc	DMSO	3
9	6	KOAc	DMF	54
10	7	KOAc	DMAc	79
11	8	KOAc	DMAc	62
12	9	KOAc	DMAc	54

[1] The runs were carried out at 120 °C for 1 h using a base (0.32 mmol), bromoacetophenone (**11a**; 30 µL, 0.25 mmol), 2-butylfuran (**10a**; 42 µL, 0.30 mmol), solvent (1 mL) and palladium complex (2.5 µmol, 1 mol%). [2] The conversions were determined by GC using decane (0.025 mL) as the internal reference.
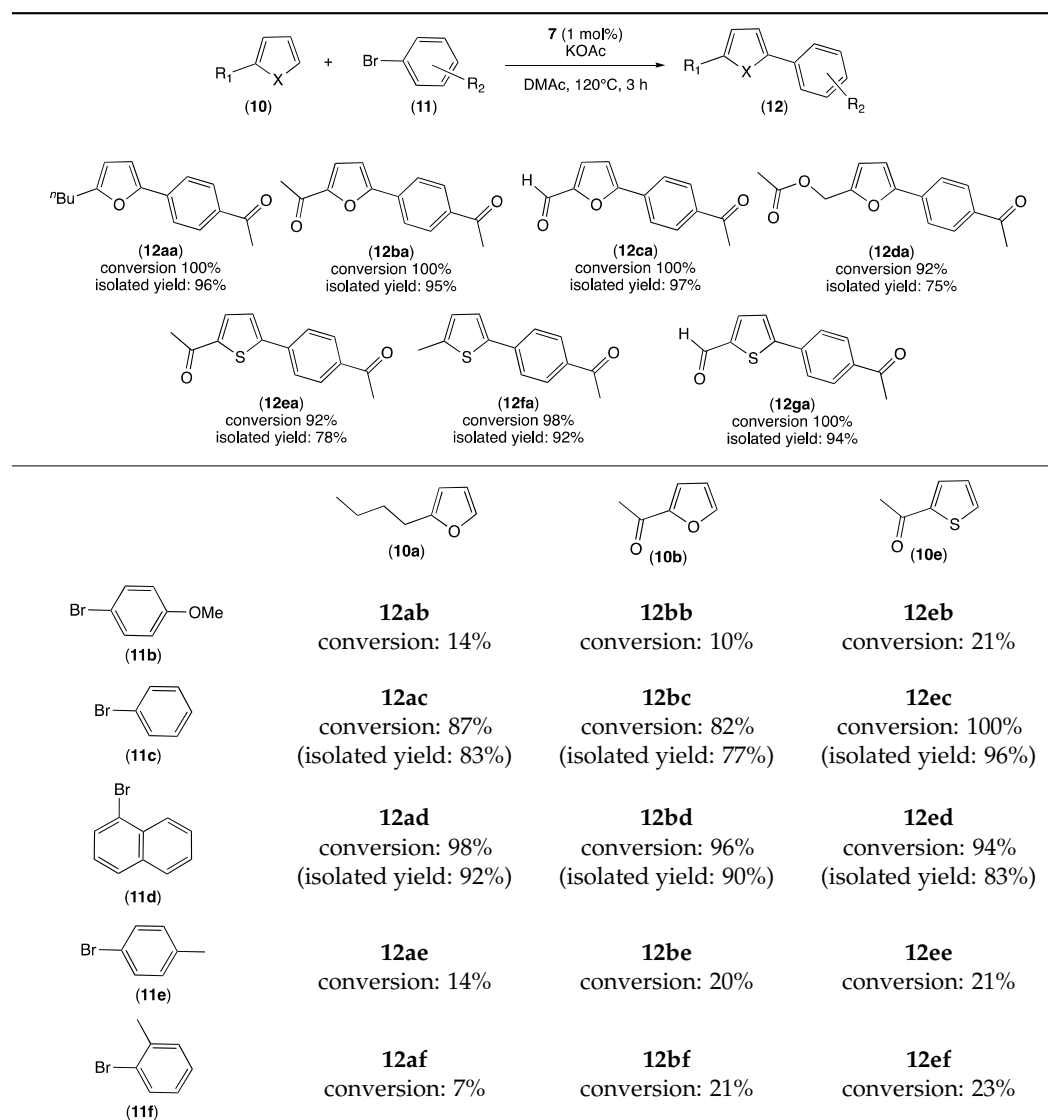
Finally, the four Pd(II) complexes were ranked. It has been shown that complexes with an F atom (complexes **8** and **9**) are less efficient than their non-fluorinated counterparts (complexes **6** and **7**) (Table 1, entries 6 and 10–12). We can note that the most active complex has the *trans* configuration of the styryl substituent (complex **7**: 79%). It is quite conceivable that during the test realized at 120 °C, an isomerization of the *cis* double bond of the styryl substituent, complex **6**, was performed, ultimately generating the same active species formed starting from complex **7**. The slightly superior efficiency of the (*E*)-complex **7** compared to the (*Z*)-complex **6** can be explained by this additional activation step, the isomerization of *cis*-styryl into *trans*-styryl, in the case of (*Z*)-complex **6**.

Having determined the optimized catalytic conditions, the cross-coupling reaction was carried out between 2-butylfuran (**10a**), 1-(2-furanyl)-ethanone (**10b**), furfural (**10c**), furfuryl acetate (**10d**), 1-(2-thienyl)-ethanone (**10e**), 2-methylthiophene (**10f**) or thenaldehyde (**10g**) and six aryl bromides, namely 4-bromoacetophenone (**11a**), 4-bromoanisole (**11b**), bromobenzene (**11c**), 1-bromonaphthalene (**11d**), 4-bromotoluene (**11e**) and 2-bromotoluene (**11f**) (Table 2). The runs were carried out using the more efficient pre-catalyst **7** (1 mol%) in DMAc for 3 h at 120 °C.

High conversions, with isolated yields in the range of 75–97%, were observed when 4-bromoacetophenone (**11a**) was employed as a coupling agent with the seven heteroarenes **10a**–**g**. The lowest heteroarylation was observed, with a conversion of 92%, when furfuryl acetate (**10d**) and 1-(2-thienyl)-ethanone (**10e**) were engaged in a cross-coupling reaction. Full conversions were measured when 2-butylfuran (**10a**), 1-(2-furanyl)-ethanone (**10b**), furfural (**10c**) and thenaldehyde (**10g**) were reacted.

In contrast to previous studies by the group of Özdemir involving alkyl substituents (for example, benzhydryl [35], 1,3-dioxalane-2-yl [38], 2-morpholinoethyl [43] or 2-morpholinoethyl [33]), instead of the styryl group on the benzimidazolylidene ligand, low conversions in the range of 10 to 21% were observed when 4-bromoanisole (**11b**) or 4-bromotoluene (**11e**) was employed. Repeating the runs with the sterically more crowded 2-bromotoluene (**11f**) did not profoundly alter the reactivity of the catalytic system, and conversions of 7–23% were measured.

On the other hand, excellent reactivities were observed when the three furanyl or thiofuranyl substrates were reacted with bromobenzene (**11c**) and 1-bromonaphthalene (**11d**), and conversions in the ranges of 82–100% and 94–98%, respectively, were measured.

Table 2. Palladium-catalyzed cross-coupling reactions between furanyl or thiofuranyl substrates and various aryl bromides [1].

(10a)

(10b)

(10e)

	10a	10b	10e
11b (Br—OMe)	**12ab** conversion: 14%	**12bb** conversion: 10%	**12eb** conversion: 21%
11c (Br—)	**12ac** conversion: 87% (isolated yield: 83%)	**12bc** conversion: 82% (isolated yield: 77%)	**12ec** conversion: 100% (isolated yield: 96%)
11d (Br-naphthyl)	**12ad** conversion: 98% (isolated yield: 92%)	**12bd** conversion: 96% (isolated yield: 90%)	**12ed** conversion: 94% (isolated yield: 83%)
11e (Br—Me)	**12ae** conversion: 14%	**12be** conversion: 20%	**12ee** conversion: 21%
11f (Br—Me ortho)	**12af** conversion: 7%	**12bf** conversion: 21%	**12ef** conversion: 23%

[1] The runs were carried out at 120 °C for 3 h using KOAc (31 mg, 0.32 mmol), aryl bromide (0.25 mmol), furanyl and thiofuranyl substrate (0.30 mmol), solvent (1 mL) and complex **6** (1.4 mg, 2.5 μmol, 1 mol%). The conversions were determined by GC using decane (0.025 mL) as the internal reference.

3. Materials and Methods

All reactions involving organometallic derivatives were carried out under an inert atmosphere of argon with dried solvents. Routine ^{1}H and ^{13}C{^{1}H} spectra were recorded with a 500 MHz Bruker Avance III spectrometer (Billerica, MA, USA). Chemical shifts and coupling constants are reported in ppm and Hz, respectively. The spectra were calibrated according to the residual protonated solvent (in CDCl$_3$ δ = 7.26 and 77.16 ppm for ^{1}H and ^{13}C{^{1}H}, respectively, or in DMSO-d$_6$ δ = 2.50 and 39.52 ppm for ^{1}H and ^{13}C{^{1}H}, respectively). ^{19}F NMR spectroscopic data are given relative to external CCl$_3$F. Mass spectra were recorded on a Bruker MicroTOF spectrometer (ESI-TOF). The catalytic solutions were analyzed by using a Varian 3900 GC equipped with a WCOT fused-silica column (25 m × 0.25 mm). Infrared spectra were recorded on a Bruker FT-IR Alpha-P spectrometer. Elemental analyses were carried out by the Service de Microanalyse, Institut de Chimie, Université de Strasbourg. (*Z*)-1-Styryl-benzimidazole (**1**) [48] and (*E*)-1-styryl-benzimidazole (**2**) [49] were prepared according to the procedures in the literature.

3.1. The General Procedure for the Synthesis of Benzimidazolium Slats

1-Styryl-benzimidazole **1** or **2** (220 mg, 1 mmol) and benzyl chloride (1 mmol) were dissolved in DMF (5 mL). The resulting solution was heated at 80 °C for 24 h. After cooling to room temperature, the salt was precipitated by the addition of Et_2O (100 mL). The white solid was filtered, washed with Et_2O (2 × 10 mL) and dried under a vacuum.

3.1.1. (Z)-1-Styryl-3-benzyl-benzimidazolium Chloride (**3**)

Yield: 73%; FT-IR: ν(CN) 1546 cm^{-1}; ^{1}H NMR (500 MHz, CDCl$_3$): δ = 11.49 (s, 1H, NC*H*N), 7.61 (dt, 1H, arom CH, $^3J_{HH}$ = 8.0 Hz, $^4J_{HH}$ = 1.0 Hz), 7.49–7.44 (m, 3H, CH arom), 7.40 (td, 1H, arom CH, $^3J_{HH}$ = 8.0 Hz, $^4J_{HH}$ = 1.0 Hz), 7.36–7.32 (m, 3H, CH arom), 7.29 (d, 1H, arom CH, $^3J_{HH}$ = 8.5 Hz), 7.25 (d, 1H, NC*H*=CHPh, $^3J_{HH}$ = 8.5 Hz), 7.21 (tt, 1H, arom CH, $^3J_{HH}$ = 7.5 Hz, $^4J_{HH}$ = 1.2 Hz), 7.13 (tt, 2H, arom CH, $^3J_{HH}$ = 7.5 Hz, $^4J_{HH}$ = 1.2 Hz), 7.08 (d, 1H, NCH=C*H*Ph, $^3J_{HH}$ = 8.5 Hz), 6.93 (d, 2H, arom CH, $^3J_{HH}$ = 7.5 Hz), 6.03 (s, 2H, NCH$_2$); ^{13}C{^{1}H} NMR (126 MHz, CDCl$_3$): δ = 143.72 (s, NCHN), 133.97 (s, NCH=CHPh), 133.04, 131.75, 130.93, 130.74, 129.68, 129.44, 129.27, 129.18, 128.56, 128.45, 127.42, 127.402, 114.31, 113.88 (14 s, arom Cs), 118.65 (s, NCH=CHPh), 51.75 (s, NCH$_2$) ppm. Elemental analysis (%): calcd for C$_{22}$H$_{19}$N$_2$Cl (346.85): C: 76.18; H: 5.52; N: 8.08; found C: 76.35; H: 5.63 N: 8.01.

3.1.2. (Z)-1-Styryl-3-(3-fluorobenzyl)-benzimidazolium Chloride (**4**)

Yield: 59%; FT-IR: ν(CN) 1547 cm^{-1}; ^{1}H NMR (500 MHz, DMSO-d$_6$): δ = 10.12 (s, 1H, NC*H*N), 8.00 (dt, 1H, arom CH, $^3J_{HH}$ = 8.0 Hz, $^4J_{HH}$ = 1.0 Hz), 7.66–7.58 (m, 3H, CH arom), 7.49–7.44 (m, 1H, CH arom), 7.35 (dt, 1H, arom CH, $^3J_{HH}$ = 10.0 Hz, $^4J_{HH}$ = 2.0 Hz), 7.31 (dt, 1H, arom CH, $^3J_{HH}$ = 8.0 Hz, $^4J_{HH}$ = 1.2 Hz), 7.28 (d, 1H, NC*H*=CHPh, $^3J_{HH}$ = 7.5 Hz), 7.27–7.26 (m, 2H, CH arom), 7.25–7.20 (m, 2H, arom CH), 7.23 (d, 1H, NCH=C*H*Ph, $^3J_{HH}$ = 7.5 Hz), 7.09–7.07 (m, 2H, CH arom), 5.82 (s, 2H, NCH$_2$); ^{13}C{^{1}H} NMR (126 MHz, DMSO-d$_6$): δ = 162.38 (d, CF arom, $^1J_{CF}$ = 245.2 Hz), 142.94 (s, NCHN), 136.53 (d, Cquat arom, $^3J_{CF}$ = 7.7 Hz), 132.52, 132.07, 130.62, 130.60, 129.47, 129.12, 128.63, 127.56, 114.19, 114.18 (10 s, arom Cs), 131.27 (d, CH arom, $^3J_{CF}$ = 8.3 Hz), 127.40 (s, NCH=CHPh), 124.50 (d, CH arom, $^4J_{CF}$ = 2.8 Hz), 119.20 (s, NCH=CHPh), 115.90 (d, CH arom, $^2J_{CF}$ = 20.8 Hz), 115.34 (d, CH arom, $^2J_{CF}$ = 22.4 Hz), 49.58 (d, NCH$_2$, $^4J_{CF}$ = 1.9 Hz); ^{19}F{^{1}H} NMR (282 MHz, DMSO-d$_6$): δ = −112.10 (s, CF arom) ppm. Elemental analysis (%): calcd for C$_{22}$H$_{18}$N$_2$FCl (364.84): C: 72.43; H: 4.97; N: 7.68; found C: 72.51; H: 5.02 N: 7.64.

3.1.3. (E)-1-Styryl-3-(3-fluorobenzyl)-benzimidazolium Chloride (**5**)

Yield: 61%; FT-IR: ν(CN) 1555 cm^{-1}; ^{1}H NMR (500 MHz, DMSO-d$_6$): δ = 10.74 (s, 1H, NC*H*N), 8.42 (dt, 1H, arom CH, $^3J_{HH}$ = 8.5 Hz, $^4J_{HH}$ = 0.7 Hz), 8.27 (d, 1H, NC*H*=CHPh, $^3J_{HH}$ = 14.5 Hz), 7.98 (dt, 1H, arom CH, $^3J_{HH}$ = 8.0 Hz, $^4J_{HH}$ = 1.0 Hz), 7.77–7.74 (m, 3H, CH arom), 7.70 (td, 1H, arom CH, $^3J_{HH}$ = 8.0 Hz, $^4J_{HH}$ = 1.0 Hz), 7.61 (d, 1H, NCH=C*H*Ph, $^3J_{HH}$ = 14.5 Hz), 7.56–7.53 (m, 1H, CH arom), 7.51–7.46 (m, 4H, CH arom), 7.42 (tt, 1H, arom CH, $^3J_{HH}$ = 7.5 Hz, $^4J_{HH}$ = 1.2 Hz), 7.25–7.21 (m, 1H, CH arom), 5.88 (s, 2H, NCH$_2$); ^{13}C{^{1}H} NMR (126 MHz, DMSO-d$_6$): δ = 162.28 (d, CF arom, $^1J_{CF}$ = 244.9 Hz), 141.00 (s, NCHN), 136.31 (d, Cquat arom, $^3J_{CF}$ = 7.7 Hz), 133.29, 130.63, 130.55, 129.19, 129.03, 127.27, 127.21, 127.16, 114.25, 113.97 (10 s, arom Cs), 131.00 (d, CH arom, $^3J_{CF}$ = 8.3 Hz), 126.35 (s, NCH=CHPh), 124.61 (d, CH arom, $^4J_{CF}$ = 2.9 Hz), 120.12 (s, NCH=CHPh), 115.68 (d, CH arom, $^2J_{CF}$ = 20.9 Hz), 115.45 (d, CH arom, $^2J_{CF}$ = 22.4 Hz), 49.63 (d, NCH$_2$, $^4J_{CF}$ = 2.0 Hz); ^{19}F{^{1}H} NMR (282 MHz, DMSO-d$_6$): δ = −112.28 (s, CF arom) ppm. Elemental analysis (%): calcd for C$_{22}$H$_{18}$N$_2$FCl (364.84): C: 72.43; H: 4.97; N: 7.68; found C: 72.53; H: 4.99 N: 7.72.

3.2. The General Procedure for the Synthesis of Palladium(II) Complexes

Benzimidazole salt (0.5 mmol) and [PdCl$_2$] (88 mg, 0.5 mmol) were added to a stirred suspension of K$_2$CO$_3$ (345 mg, 2.5 mmol) in pyridine (5 mL). The resulting reaction mixture was stirred at 80 °C for 4 h, except for the synthesis of complex **7**, for which the reaction mixture was heated to 120 °C. After cooling to room temperature, the pyridine was removed

under a vacuum. The solid residue was dissolved in CH_2Cl_2 (10 mL), and the mixture was filtered through Celite. After the evaporation of the solvent, the crude solid was purified by flash chromatography (CH_2Cl_2 as eluent) to afford the yellow palladium(II) complex.

3.2.1. *trans*-Dichloro-[(*Z*)-1-styryl-3-benzyl-benzimidazol-2-yliden]pyridine Palladium(II) (**6**)

Yield: 66%; FT-IR: ν(CN) 1446 cm^{-1}; ^{1}H NMR (500 MHz, CDCl$_3$): δ = 9.04 (dt, 2H, arom CH, $^3J_{HH}$ = 5.0 Hz, $^4J_{HH}$ = 1.5 Hz), 7.77 (tt, 1H, arom CH, $^3J_{HH}$ = 7.7 Hz, $^4J_{HH}$ = 1.7 Hz), 7.67 (d, 1H, NC*H*=CHPh, $^3J_{HH}$ = 8.5 Hz), 7.64–7.62 (m, 2H, CH arom), 7.40–7.32 (m, 5H, arom CH), 7.24–7.22 (m, 2H, CH arom), 7.13–7.10 (m, 3H, CH arom), 7.07 (dt, 1H, arom CH, $^3J_{HH}$ = 8.0 Hz, $^4J_{HH}$ = 1.0 Hz), 7.00 (d, 1H, NCH=C*H*Ph, $^3J_{HH}$ = 8.5 Hz), 6.99 (td, 1H, arom CH, $^3J_{HH}$ = 7.7 Hz, $^4J_{HH}$ = 1.0 Hz), 6.90 (td, 1H, arom CH, $^3J_{HH}$ = 7.7 Hz, $^4J_{HH}$ = 1.0 Hz), 6.80 (dt, 1H, arom CH, $^3J_{HH}$ = 8.0 Hz, $^4J_{HH}$ = 1.0 Hz), 6.26 (s, 2H, NCH$_2$); ^{13}C{^{1}H} NMR (126 MHz, CDCl$_3$): δ = 165.15 (s, NCN), 151.42, 138.30, 134.94, 133.88, 133.69, 133.35, 129.06, 128.95, 128.63, 128.51, 128.42, 124.63, 123.40, 123.35, 123.31, 112.54, 111.36 (17 s, arom Cs), 129.65 (s, NCH=*C*HPh), 128.16 (s, N*C*H=CHPh), 53.47 (s, NCH$_2$) ppm. MS (ESI-TOF): m/z = 530.06 [M − Cl]$^+$ (expected isotopic profiles). Elemental analysis (%): calcd for C$_{27}$H$_{23}$N$_3$PdCl$_2$ (566.82): C: 57.21; H: 4.09; N: 7.41; found C: 57.14; H: 3.96 N: 7.35.

3.2.2. *trans*-Dichloro-[(*E*)-1-styryl-3-benzyl-benzimidazol-2-yliden]pyridine Palladium(II) (**7**)

Yield: 61%; FT-IR: ν(CN) 1446 cm^{-1}; ^{1}H NMR (500 MHz, CDCl$_3$): δ = 8.98 (dt, 2H, arom CH, $^3J_{HH}$ = 5.0 Hz, $^4J_{HH}$ = 1.5 Hz), 8.32 (d, 1H, NC*H*=CHPh, $^3J_{HH}$ = 14.5 Hz), 7.77 (tt, 1H, arom CH, $^3J_{HH}$ = 7.5 Hz, $^4J_{HH}$ = 1.5 Hz), 7.70–7.62 (m, 5H, CH arom), 7.60 (d, 1H, NCH=C*H*Ph, $^3J_{HH}$ = 14.5 Hz), 7.45 (tt, 2H, arom CH, $^3J_{HH}$ = 7.2 Hz, $^4J_{HH}$ = 1.7 Hz), 7.40–7.35 (m, 6H, arom CH), 7.31–7.27 (m, 1H, CH arom), 7.20–7.14 (m, 2H, CH arom), 6.29 (s, 2H, NCH$_2$); ^{13}C{^{1}H} NMR (126 MHz, CDCl$_3$): δ = 165.48 (s, NCN), 151.45, 138.31, 134.82, 134.62, 134.58, 134.32, 129.09, 128.81, 128.75, 128.57, 128.47, 128.17, 127.24, 124.70, 124.04, 111.88, 111.82 (17 s, arom Cs), 129.08 (s, NCH=*C*HPh), 124.80 (s, N*C*H=CHPh), 53.66 (s, NCH$_2$) ppm. MS (ESI-TOF): m/z = 566.04 [M + H]$^+$ (expected isotopic profiles). Elemental analysis (%): calcd for C$_{27}$H$_{23}$N$_3$PdCl$_2$ (566.82): C: 57.21; H: 4.09; N: 7.41; found C: 57.16; H: 3.99 N: 7.38.

3.2.3. *trans*-Dichloro-[(*Z*)-1-styryl-3-(3-fluorobenzyl)-benzimidazol-2-yliden]pyridine Palladium(II) (**8**)

Yield: 67%; FT-IR: ν(CN) 1446 cm^{-1}; ^{1}H NMR (300 MHz, CDCl$_3$): δ = 9.03 (dt, 2H, arom CH, $^3J_{HH}$ = 4.8 Hz, $^4J_{HH}$ = 1.5 Hz), 7.78 (tt, 1H, arom CH, $^3J_{HH}$ = 7.6 Hz, $^4J_{HH}$ = 1.5 Hz), 7.66 (d, 1H, NC*H*=CHPh, $^3J_{HH}$ = 9.0 Hz), 7.41–7.31 (m, 5H, CH arom), 7.25–7.21 (m, 2H, arom CH), 7.15–7.10 (m, 3H, CH arom), 7.06–6.99 (m, 3H, CH arom), 7.02 (d, 1H, NCH=C*H*Ph, $^3J_{HH}$ = 9.0 Hz), 6.96–6.95 (m, 1H, arom CH), 6.82 (dt, 1H, arom CH, $^3J_{HH}$ = 8.1 Hz, $^4J_{HH}$ = 0.9 Hz), 6.24 (s, 2H, NCH$_2$); ^{13}C{^{1}H} NMR (126 MHz, CDCl$_3$): δ = 165.59 (s, NCN), 163.23 (d, CF arom, $^1J_{CF}$ = 247.6 Hz), 151.43, 138.36, 133.74, 133.63, 133.37, 128.94, 128.67, 128.59, 124.67, 123.57, 123.55, 112.67, 111.13 (13 s, arom Cs), 137.60 (d, Cquat arom, $^3J_{CF}$ = 7.4 Hz), 130.69 (d, CH arom, $^3J_{CF}$ = 8.3 Hz), 129.91 (s, NCH=*C*HPh), 123.72 (d, CH arom, $^4J_{CF}$ = 2.9 Hz), 123.22 (s, N*C*H=CHPh), 115.50 (d, CH arom, $^2J_{CF}$ = 21.2 Hz), 115.25 (d, CH arom, $^2J_{CF}$ = 22.5 Hz), 52.81 (d, NCH$_2$, $^4J_{CF}$ = 1.9 Hz); ^{19}F{^{1}H} NMR (282 MHz, CDCl$_3$): δ = −111.89 (s, CF arom) ppm. MS (ESI-TOF): m/z = 548.05 [M − Cl]$^+$ (expected isotopic profiles). Elemental analysis (%): calcd for C$_{27}$H$_{22}$N$_3$FPdCl$_2$ (584.81): C: 55.45; H: 3.79; N: 7.19; found C: 55.31; H: 3.67 N: 7.04.

3.2.4. *trans*-Dichloro-[(*E*)-1-styryl-3-(3-fluorobenzyl)-benzimidazol-2-yliden]pyridine Palladium(II) (**9**)

Yield: 65%; FT-IR: ν(CN) 1446 cm^{-1}; ^{1}H NMR (300 MHz, CDCl$_3$): δ = 8.97 (dt, 2H, arom CH, $^3J_{HH}$ = 5.0 Hz, $^4J_{HH}$ = 1.5 Hz), 8.29 (d, 1H, NC*H*=CHPh, $^3J_{HH}$ = 14.5 Hz), 7.77 (tt, 1H, arom CH, $^3J_{HH}$ = 7.7 Hz, $^4J_{HH}$ = 1.7 Hz), 7.70 (dt, 1H, arom CH, $^3J_{HH}$ = 8.0 Hz,

$^4J_{HH}$ = 1.0 Hz), 7.67–7.64 (m, 2H, CH arom), 7.61 (d, 1H, NCH=C*H*Ph, $^3J_{HH}$ = 14.5 Hz), 7.45 (tt, 2H, arom CH, $^3J_{HH}$ = 7.5 Hz, $^4J_{HH}$ = 1.7 Hz), 7.41–7.38 (m, 2H, arom CH), 7.37–7.32 (m, 4H, CH arom), 7.32–7.30 (m, 1H, CH arom), 7.21 (td, 1H, arom CH, $^3J_{HH}$ = 7.7 Hz, $^4J_{HH}$ = 1.0 Hz), 7.15 (dt, 1H, arom CH, $^3J_{HH}$ = 8.0 Hz, $^4J_{HH}$ = 1.0 Hz), 7.04–7.00 (m, 1H, arom CH), 6.27 (s, 2H, NCH$_2$); ^{13}C{^{1}H} NMR (126 MHz, CDCl$_3$): δ = 165.87 (s, NCN), 163.23 (d, CF arom, $^1J_{CF}$ = 247.7 Hz), 151.43, 138.36, 134.58, 134.53, 134.16, 130.74, 130.68, 129.09, 127.26, 124.72, 124.63, 124.22, 111.94, 111.61 (14 s, arom Cs), 137.30 (d, Cquat arom, $^3J_{CF}$ = 7.3 Hz), 130.71 (d, CH arom, $^3J_{CF}$ = 8.2 Hz), 128.89 (s, NCH=CHPh), 124.21 (s, NCH=CHPh), 123.73 (d, CH arom, $^4J_{CF}$ = 3.0 Hz), 115.54 (d, CH arom, $^2J_{CF}$ = 21.2 Hz), 115.27 (d, CH arom, $^2J_{CF}$ = 22.6 Hz), 52.98 (d, NCH$_2$, $^4J_{CF}$ = 1.9 Hz); ^{19}F{^{1}H} NMR (282 MHz, CDCl$_3$): δ = −111.84 (s, CF arom) ppm. MS (ESI-TOF): m/z = 548.05 [M − Cl]$^+$ (expected isotopic profiles). Elemental analysis (%): calcd for C$_{27}$H$_{22}$N$_3$FPdCl$_2$ (584.81): C: 55.45; H: 3.79; N: 7.19; found C: 55.38; H: 3.73 N: 7.12.

3.3. The General Procedure for the Palladium-Catalyzed C–H Activation

A 5 mL vial under an argon atmosphere was filled with KOAc (32 mg, 0.32 mmol), aryl bromide (0.25 mmol), furan or thiofurane derivative (0.30 mmol), decane (0.025 mL, internal reference) and a solution of palladium complex (2.5 µmol, 1 mol%) in DMAc (1 mL). Then, the reaction mixture was heated at 120 °C for 3 h. After cooling to room temperature, the crude reaction was passed through a Millipore filter and analyzed by GC. All products were unambiguously identified by NMR after their isolation.

3.4. X-ray Crystal Structure Analysis

The slow diffusion of Et$_2$O into a CH$_2$Cl$_2$ solution of palladium complexes **6**, **8** and **9** led to the formation of single crystals suitable for an X-ray analysis. The analysis was carried out on a Bruker APEX II DUO Kappa-CCD diffractometer for complexes **6** and **8** or a Bruker Photon III CPAD diffractometer for complex **9** using Mo-Kα radiation (λ = 0.71073 Å). The structures were solved using the SHELXT-2018 program [50]. The refinement and all further calculations were carried out using SHELXL-2019 [51]. The H-atoms were included in the calculated positions and treated as riding atoms using SHELXL default parameters. The non-H atoms were refined anisotropically using weighted full-matrix least-squares on F^2. The data collection and structure refinement details are given in Table 3.

Table 3. Crystal data and structure refinement parameters for palladium(II) complexes **6**, **8** and **9**.

Complex		6	8	9
CCDC depository		2343643	2343644	2343645
color/shape		colorless/block	yellow/prism	colorless/block
chemical formula		C$_{27}$H$_{23}$Cl$_2$N$_3$Pd	C$_{27}$H$_{22}$FCl$_2$N$_3$Pd	C$_{27}$H$_{22}$FCl$_2$N$_3$Pd
molecular weight (g mol^{-1})		566.78	584.77	584.77
crystal system		orthorhombic	orthorhombic	monoclinic
space group		P2$_1$2$_1$2$_1$	P2$_1$2$_1$2$_1$	C2/c
	a (Å)	9.788(5)	9.7942(8)	22.5267(19)
	b (Å)	14.022(8)	14.2926(11)	16.6782(13)
unit cell	c (Å)	18.219(9)	17.9496(18)	14.5980(11)
parameters	α (°)	90	90	90
	β (°)	90	90	117.218(4)
	γ (°)	90	90	90
volume (Å^3)		2500(2)	2512.7(4)	4877.2(7)
Z		4	4	8
D (g cm^{-3})		1.506	1.546	1.593
μ (mm^{-1})		0.976	0.979	1.009
T_{min}, T_{max}		0.4111, 0.7456	0.908, 0.944	0.6803, 0.7456
F(000)		1144	1176	2352

Table 3. *Cont.*

Complex	6	8	9
crystal size (mm)	$0.180 \times 0.160 \times 0.140$	$0.100 \times 0.080 \times 0.060$	$0.120 \times 0.100 \times 0.100$
index ranges	$-12 \leq h \leq 12$	$-12 \leq h \leq 12$	$-29 \leq h \leq 29$
	$-18 \leq k \leq 18$	$-18 \leq k \leq 18$	$-21 \leq k \leq 21$
	$-21 \leq l \leq 23$	$-20 \leq l \leq 23$	$-19 \leq l \leq 16$
θ range for data collection (°)	$1.833 \leq \theta \leq 27.827$	$1.821 \leq \theta \leq 28.071$	$1.589 \leq \theta \leq 27.975$
reflections collected	24,049	24,519	31,543
independent/observed	5925/4777	6076/4425	5850/4256
R_{int}	0.1000	0.0954	0.0822
data/restraints/parameters	5925/0/298	6076/0/307	5850/0/316
goodness-of-fit on F^2	1.005	0.978	1.018
final R indices ($I > 2.0\,\sigma(I)$)	$R_1 = 0.0500$, $wR_2 = 0.1157$	$R_1 = 0.0467$, $wR_2 = 0.0765$	$R_1 = 0.0525$, $wR_2 = 0.1290$
R indices (all data)	$R_1 = 0.0710$, $wR_2 = 0.1299$	$R_1 = 0.0800$, $wR_2 = 0.0879$	$R_1 = 0.0790$, $wR_2 = 0.1451$
$\Delta\rho_{max}$, $\Delta\rho_{min}$ (eÅ^{-3})	1.379, -0.990	0.549, -0.570	2.181, -0.945
Flack parameter	0.07(4)	$-0.04(4)$	/

4. Conclusions

In this article, we reported the synthesis of four NHC-Pd(II) complexes derived from (*Z*)- or (*E*)-styryl-*N*-alkylbenzimidazolium salts. During the formation of the latter organometallic compounds, the *cis* or *trans* configuration of the double bond of the styryl substituent depends on the temperature of the reaction. In fact, a temperature of 120 °C resulted in the isomerization of the *cis* double-bond of the benzimidazolium salt into the *trans* configuration in the resulting Pd(II) complex. These Pd(II) complexes were fully characterized using spectroscopic methods, and for three of them, a single-crystal X-ray diffraction study was carried out. The catalytic abilities of these Pd(II) pre-catalysts to form carbon-carbon bonds via the C–H activation of the furanyl and thiofuranyl derivatives were investigated. After the optimization of the catalytic conditions using DMAc and KOAc as bases for 3 h at 120 °C, full or quasi-full conversions were observed in the arylation of seven heteroaryls with 4-bromoacetophenone or when bromobenzene and 1-bromonaphthalene were reacted with 2-butylfuran, 1-(2-furanyl)-ethanone or 1-(2-thiephyl)-ethanone.

Future works will aim to exploit this thermal modification, the isomerization of a double bond from *cis* to *trans* configuration, of the coordination sphere of the catalytic center in cross-coupling reactions.

Supplementary Materials: The following supporting information can be downloaded at https://www.mdpi.com/article/10.3390/inorganics12060175/s1. Characterizing data of (*Z*)-1-styryl-3-benzyl-benzimidazolium chloride (**3**), Figure S1. FT-IR spectrum, Figure S2. ^{1}H NMR spectrum (CDCl$_3$)and ^{13}C{^{1}H} NMR spectrum (CDCl$_3$), Figure S3. Characterizing data of (*Z*)-1-styryl-3-(3-fluorobenzyl)-benzimidazolium chloride (**4**), Figure S4. FT-IR spectrum, Figure S5. ^{1}H NMR spectrum (DMSO-d6), Figure S6. ^{13}C{^{1}H} NMR spectrum (DMSO-d$_6$), Figure S7. ^{19}F{^{1}H} NMR spectrum (DMSO-d$_6$) and characterizing data of (*E*)-1-styryl-3-(3-fluorobenzyl)-benzimidazolium chloride (**5**), Figure S8. FT-IR spectrum, Figure S9. ^{1}H NMR spectrum (DMSO-d$_6$), Figure S10. ^{13}C{^{1}H} NMR spectrum (DMSO-d$_6$), Figure S11. ^{19}F{^{1}H} NMR spectrum (DMSO-d$_6$) and characterizing data of *trans*-dichloro-[(*Z*)-1-styryl-3-benzyl-benzimidazol-2-yliden]pyridine palladium(II) (**6**), Figure S12. FT-IR spectrum, Figure S13. Mass spectrum (ESI-TOF), Figure S14. ^{1}H NMR spectrum (CDCl3), Figure S15. ^{13}C{^{1}H} NMR spectrum (CDCl$_3$) and characterizing data of *trans*-dichloro-[(*E*)-1-styryl-3-benzyl-benzimidazol-2-yliden]pyridine palladium(II) (**7**), Figure S16. FT-IR spectrum, Figure S17. Mass spectrum (ESI-TOF), Figure S18. ^{1}H NMR spectrum (CDCl$_3$), Figure S19. ^{13}C{^{1}H} NMR spectrum (CDCl$_3$) and characterizing data of *trans*-dichloro-[(*Z*)-1-styryl-3-(3-fluorobenzyl)-benzimidazol-2-yliden]pyridine palladium(II) (**8**), Figure S20. FT-IR spectrum, Figure S21. Mass spectrum (ESI-TOF), Figure S22. ^{1}H NMR spectrum (CDCl$_3$), Figure S23. ^{13}C{^{1}H} NMR spectrum (CDCl$_3$), Figure S24. ^{19}F{^{1}H} NMR spectrum (CDCl$_3$) and characterizing data of *trans*-dichloro-[(*E*)-1-styryl-3-(3-fluorobenzyl)-benzimidazol-2-yliden]pyridine palladium(II) (**9**), Figure S25. FT-IR spectrum, Figure S26. Mass spectrum (ESI-TOF), Figure S27. ^{1}H NMR spectrum (CDCl3), Figure S28. ^{13}C{^{1}H} NMR

spectrum (CDCl$_3$), Figure S29. ^{19}F{^{1}H} NMR spectrum (CDCl$_3$) and ^{1}H NMR description of the catalytic products.

Author Contributions: Conceptualization, N.Ş. and D.S.; methodology, N.Ş. and D.S.; validation, N.Ş. and D.S.; formal analysis, N.Ş. and D.S.; investigation, N.Ş.; resources, D.S.; data curation, N.Ş. and D.S.; writing—original draft preparation, N.Ş.; writing—review and editing, D.S.; supervision, İ.Ö. All authors have read and agreed to the published version of the manuscript.

Data Availability Statement: The raw data supporting the conclusions of this article will be made available by the authors on request.

Conflicts of Interest: The authors declare no conflicts of interest.

References

1. Zhao, Q.; Meng, G.; Nolan, S.P.; Szostak, M. *N*-Heterocyclic carbene complexes in C-H activation reactions. *Chem. Rev.* **2020**, *120*, 1981–2048. [CrossRef]
2. Rogge, T.; Kaplaneris, N.; Chatani, N.; Kim, J.; Chang, S.; Punji, B.; Schafer, L.L.; Musaev, D.G.; Wencel-Delord, J.; Roberts, C.A.; et al. C-H activation. *Nat. Rev. Dis. Primers* **2021**, *1*, 43. [CrossRef]
3. Dalton, T.; Faber, T.; Glorius, F. C-H activation: Toward sustainability and applications. *ACS Cent. Sci.* **2021**, *7*, 245–261. [CrossRef] [PubMed]
4. Thombal, R.S.; Rubio, P.Y.M.; Lee, D.; Maiti, D.; Lee, Y.R. Modern palladium-catalyzed transformations involving C-H activation and subsequent annulation. *ACS Catal.* **2022**, *12*, 5217–5230. [CrossRef]
5. Oi, S.; Fukita, S.; Hirata, N.; Watanuki, N.; Miyano, S.; Inoue, Y. Ruthenium complex-catalyzed direct ortho arylation and alkenylation of 2-arylpyridines with organic halides. *Org. Lett.* **2001**, *3*, 2579–2581. [CrossRef] [PubMed]
6. Lewis, J.C.; Wiedemann, S.H.; Bergman, R.G.; Ellman, J.A. Arylation of heterocycles via rhodium-catalyzed C-H bond functionalization. *Org. Lett.* **2004**, *6*, 35–38. [CrossRef] [PubMed]
7. Campeau, L.-C.; Thansandote, P.; Fagnou, K. High-yielding intramolecular direct arylation reactions with aryl chlorides. *Org. Lett.* **2005**, *7*, 1857–1860. [CrossRef]
8. Yang, L.; Yuan, J.; Mao, P.; Guo, Q. Chelating palladium complexes containing pyridine/pyrimidine hydroxyalkyl difunctionalized *N*-heterocyclic carbenes: Synthesis, structure, and catalytic activity towards C-H activation. *RSC Adv.* **2015**, *5*, 107601–107607. [CrossRef]
9. Denisov, M.S.; Dmitriev, M.V.; Gorbunov, A.A.; Glushkov, V.A. Complexes of palladium(II) with *N*-heterocyclic carbenes from adamantylimidazole as precatalysts for thiophene and imidazole arylation. *Russ. Chem. Bull.* **2019**, *68*, 2039–2047. [CrossRef]
10. Glushkov, V.A.; Denisov, M.S.; Gorbunov, A.A.; Myalitzin, Y.A.; Dmitriev, M.V.; Slepukhin, P.A. Adamantanyl-substituted PEPPSI-type palladium(II) *N*-heterocyclic carbene complexes: Synthesis and catalytic application for CH activation of substituted thiophenes. *Chem. Heterocycl. Comp.* **2019**, *55*, 217–228. [CrossRef]
11. Ma, B.-B.; Lan, X.-B.; Shen, D.-S.; Liu, F.-S.; Xu, C. Direct C-H bond (hetero)arylation of thiazole derivatives at 5-position catalyzed by *N*-heterocyclic carbene palladium complexes at low catalyst loadings under aerobic conditions. *J. Organomet. Chem.* **2019**, *897*, 13–22. [CrossRef]
12. Campeau, L.-C.; Parisien, M.; Leblanc, M.; Fagnou, K. Biaryl synthesis via direct arylation: Establishment of an efficient catalyst for intramolecular processes. *J. Am. Chem. Soc.* **2004**, *126*, 9186–9187. [CrossRef] [PubMed]
13. Erdoğan, H.; Aktaş, A.; Gök, Y.; Sarı, Y. *N*-Propylphthalimide-substituted bis-(NHC)PdX$_2$ complexes: Synthesis, characterization and catalytic activity in direct arylation reactions. *Transit. Met. Chem.* **2018**, *43*, 31–37. [CrossRef]
14. Gautama, A.; Shahini, C.R.; Siddappa, A.P.; Grzegorz, M.J.; Hemavathi, B.; Ahipa, T.N.; Srinivasa, B. Palladium(II) complexes of coumarin substituted 1,2,4-triazol-5-ylidenes for catalytic C-C cross-coupling and C-H activation reactions. *J. Organomet. Chem.* **2021**, *934*, 121540. [CrossRef]
15. Martin, A.R.; Chartoire, A.; Slawin, A.M.Z.; Nolan, S.P. Extending the utility of [Pd(NHC)(cinnamyl)Cl] precatalysts: Direct arylation of heterocycles. *Beilstein J. Org. Chem.* **2012**, *8*, 1637–1643. [CrossRef] [PubMed]
16. Ahmed, J.; Sau, S.C.; Sreejyothi, P.; Hota, P.K.; Vardhanapu, P.K.; Vijaykumar, G.; Mandal, S.K. Direct C-H arylation of heteroarenes with aryl chlorides by using an abnormal *N*-heterocyclic-carbene-palladium catalyst. *Eur. J. Org. Chem.* **2017**, *2017*, 1004–1011. [CrossRef]
17. O'Brien, C.J.; Kantchev, E.A.B.; Valente, C.; Hadei, N.; Chass, G.A.; Lough, A.; Hopkinson, A.C.; Organ, M.G. Easily prepared air- and moisture-stable Pd–NHC (NHC = N-heterocyclic carbene) complexes: A reliable, user-friendly, highly active palladium precatalyst for the Suzuki-Miyaura reaction. *Chem. Eur. J.* **2006**, *12*, 4743–4748. [CrossRef] [PubMed]
18. Valente, C.; Calimsiz, S.; Hoi, K.H.; Mallik, D.; Sayah, M.; Organ, M.G. The development of bulky palladium NHC complexes for the most-challenging cross-coupling reactions. *Angew. Chem. Int. Ed.* **2012**, *51*, 3314–3332. [CrossRef] [PubMed]

19. Vasu, G.R.P.; Venkata, K.R.M.; Kakarla, R.R.; Ranganath, K.V.S.; Aminabhavi, T.M. Recent advances in sustainable *N*-heterocyclic carbene-Pd(II)-pyridine (PEPPSI) catalysts: A review. *Environ. Res.* **2023**, *225*, 115515. [CrossRef]

20. Shaughnessy, K.H. Development of palladium precatalysts that efficiently generate LPd(0) active species. *Isr. J. Chem.* **2020**, *60*, 180–194. [CrossRef]

21. Lei, P.; Meng, G.; Ling, Y.; An, J.; Szostak, M. Pd-PEPPSI: Pd-NHC precatalyst for Suzuki-Miyaura cross-coupling reactions of amides. *J. Org. Chem.* **2017**, *82*, 6638–6646. [CrossRef] [PubMed]

22. İmik, F.; Yasar, S.; Özdemir, İ. Synthesis and investigation of catalytic activity of phenylene—And biphenylene bridged bimetallic palladium-PEPPSI complexes. *J. Organomet. Chem.* **2019**, *896*, 162–167. [CrossRef]

23. Rahman, M.M.; Zhang, J.; Zhao, Q.; Feliciano, J.; Bisz, E.; Dziuk, B.; Lalancette, R.; Szostak, R.; Szostak, M. Pd-PEPPSI *N*-heterocyclic carbene complexes from caffeine: Application in Suzuki, Heck, and Sonogashira reactions. *Organometallics* **2022**, *41*, 2281–2290. [CrossRef] [PubMed]

24. Borah, D.; Saha, B.; Sarma, B.; Das, P. A new PEPPSI type *N*-heterocyclic carbene palladium(II) complex and its efficiency as a catalyst for Mizoroki-Heck cross-coupling reactions in water. *J. Chem. Sci.* **2020**, *132*, 51. [CrossRef]

25. Organ, M.G.; Abdel-Hadi, M.; Avola, S.; Hadei, N.; Nasielski, J.; O'Brien, C.J.; Valente, C. Biaryls made easy: PEPPSI and the Kumada-Tamao-Corriu reaction. *Chem. Eur. J.* **2007**, *13*, 150–157. [CrossRef] [PubMed]

26. Valente, C.; Belowich, M.E.; Hadei, N.; Organ, M.O. Pd-PEPPSI complexes and the Negishi reaction. *Eur. J. Org. Chem.* **2010**, *2010*, 4343–4354. [CrossRef]

27. Erdemir, F.; Celepci, D.B.; Aktaş, A.; Gök, Y. 2-Hydroxyethyl-substituted (NHC)PdI$_2$(pyridine) (Pd-PEPPSI) complexes: Synthesis, characterization and the catalytic activity in the Sonogashira cross-coupling reaction. *ChemistrySelect* **2019**, *4*, 5585–5590. [CrossRef]

28. Reddy, M.V.K.; Anusha, G.; Reddy, P.V.G. Sterically enriched bulky 1,3-bis(*N*,*N*′-aralkyl)benzimidazolium based Pd-PEPPSI complexes for Buchwald-Hartwig amination reactions. *New J. Chem.* **2020**, *44*, 11694–11703. [CrossRef]

29. Huang, F.-D.; Xu, C.; Lu, D.-D.; Shen, D.-S.; Li, T.; Liu, F.-S. Pd-PEPPSI-IPentAn promoted deactivated amination of aryl chlorides with amines under aerobic conditions. *J. Org. Chem.* **2018**, *83*, 9144–9155. [CrossRef]

30. He, X.X.; Li, Y.; Ma, B.B.; Ke, Z.; Liu, F.S. Sterically encumbered tetraarylimidazolium carbene Pd-PEPPSI complexes: Highly efficient direct arylation of imidazoles with aryl bromides under aerobic conditions. *Organometallics* **2016**, *35*, 2655–2663. [CrossRef]

31. Nie, B.; Wu, W.; Ren, Q.; Wang, Z.; Zhang, J.; Zhang, Y.; Jiang, H. Access to cycloalkeno[c]-fused pyridines via Pd-catalyzed C(sp^2)-H activation and cyclization of N-acetyl hydrazones of acylcycloalkenes with vinyl azides. *Org. Lett.* **2020**, *22*, 7786–7790. [CrossRef] [PubMed]

32. Gokanapalli, A.; Motakatla, V.K.R.; Peddiahgari, V.G.R. Benzimidazole bearing Pd–PEPPSI complexes catalyzed direct C2-arylation/heteroarylation of N-substituted benzimidazoles. *Appl. Organomet. Chem.* **2020**, *34*, e5869. [CrossRef]

33. Bensalah, D.; Mansour, L.; Sauthier, M.; Gurbuz, N.; Özdemir, İ.; Beji, L.; Gatrig, R.; Hamdi, N. Plausible PEPPSI catalysts for direct C-H functionalization of five-membered heterocyclic bioactive motifs: Synthesis, spectral, X-ray crystallographic characterizations and catalytic activity. *RSC Adv.* **2023**, *13*, 31386–31410. [CrossRef] [PubMed]

34. Şahin, N.; Sémeril, D.; Brenner, E.; Matt, D.; Özdemir, İ.; Kaya, C.; Toupet, L. Resorcinarene-functionalised imidazolium salts as ligand precursors for palladium-catalysed Suzuki-Miyaura cross-couplings. *ChemCatChem* **2013**, *5*, 1116–1125. [CrossRef]

35. El-Krim Sandeli, A.; Khiri-Meribout, N.; Benzerka, S.; Boulebd, H.; Gürbüz, N.; Özdemir, N.; Özdemir, İ. Synthesis, structures, DFT calculations, and catalytic application in the direct arylation of five-membered heteroarenes with aryl bromides of novel palladium-N-heterocyclic carbene PEPPSI-type complexes. *New J. Chem.* **2021**, *45*, 17878–17892. [CrossRef]

36. Hamdi, H.; Slimani, I.; Mansour, L.; Alresheedi, F.; Gürbüz, N.; Özdemir, İ. *N*-Heterocyclic carbene-palladium-PEPPSI complexes and their catalytic activity in the direct C-H bond activation of heteroarene derivatives with aryl bromides: Synthesis, and antimicrobial and antioxidant activities. *New J. Chem.* **2021**, *45*, 21248–21262. [CrossRef]

37. Khan, S.; Buğday, N.; Yasar, S.; Ullah, N.; Özdemir, İ. Pd-*N*-heterocyclic carbene complex catalysed C-H bond activation of 2-isobutylthiazole at the C5 position with aryl bromides. *New J. Chem.* **2021**, *45*, 6281–6292. [CrossRef]

38. Lasmari, S.; Gürbüz, N.; Boulcina, R.; Özdemir, N.; Özdemir, İ. Synthesis of [PdBr$_2$(benzimidazole-2-ylidene)(pyridine)] complexes and their catalytic activity in the direct C-H bond activation of 2-substituted heterocycles. *Polyhedron* **2021**, *199*, 115091. [CrossRef]

39. Nawaz, Z.; Gürbüz, N.; Zafar, M.N.; Tahir, M.N.; Ashfaq, M.; Karci, H.; Özdemir, İ. Direct arylation (hetero-coupling) of heteroarenes via unsymmetrical palladium-PEPPSI-NHC type complexes. *Polyhedron* **2021**, *208*, 115412. [CrossRef]

40. Kaloğlu, M.; Şahan, M.H.; Düşünceli, S.D.; Özdemir, İ. Synthesis of quinoxaline-linked bis(benzimidazolium) salts and their catalytic application in palladium-catalyzed direct arylation of heteroarenes. *Catal. Lett.* **2022**, *152*, 2012–2024. [CrossRef]

41. Slimani, I.; Boubakri, L.; Özdemir, N.; Mansour, L.; Özdemir, İ.; Gürbüz, N.; Yasar, S.; Sauthier, M.; Hamdi, N. Substituted *N*-heterocyclic carbene PEPPSI-type palladium complexes with different *N*-coordinated ligands: Involvement in the direct C-H bond activation of heteroarenes derivatives with aryl bromide and their antimicrobial, anti-inflammatory and antioxidant activities. *Inorg. Chim. Acta* **2022**, *532*, 120747.

42. Munir, N.; Gürbüz, N.; Zafar, M.N.; Evren, E.; Şen, B.; Aygün, M.; Özdemir, İ. Plausible PEPPSI catalysts for direct C-H functionalization of furans and pyrroles. *J. Mol. Struct.* **2024**, *1295*, 136679. [CrossRef]

43. Touj, N.; Bensalah, D.; Mansour, L.; Sauthier, M.; Gürbüz, N.; Özdemir, İ.; Hamdi, N. Synthesis of palladium complexes containing benzimidazole core and their catalytic activities in direct C-H functionalization of five-membered heterocyclic bioactive motifs. *J. Mol. Struct.* **2024**, *1297*, 136885. [CrossRef]

44. Meng, G.; Kakalis, L.; Nolan, S.P.; Szostak, M. A simple ^{1}H NMR method for determining the σ-donor properties of *N*-heterocyclic carbenes. *Tetrahedron Lett.* **2019**, *60*, 378–781. [CrossRef]

45. Fecher, G.-H.; Kübler, J.; Felser, C. Chirality in the solid state: Chiral crystal structures in chiral and achiral space groups. *Materials* **2022**, *15*, 5812. [CrossRef] [PubMed]

46. Parsons, S.; Flack, H.D.; Wagner, T. Use of intensity quotients and differences in absolute structure refinement. *Acta Crystallogr. Sect. B* **2013**, *69*, 249–259. [CrossRef]

47. Onar, G.; Gürses, C.; Karatas, M.O.; Balcıoğlu, S.; Akbay, N.; Özdemir, N.; Ates, B.; Alıcı, B. Palladium(II) and ruthenium(II) complexes of benzotriazole functionalized *N*-heterocyclic carbenes: Cytotoxicity, antimicrobial, and DNA interaction studies. *J. Organomet. Chem.* **2019**, *886*, 48–56. [CrossRef]

48. Reddy, V.P.; Iwasaki, T.; Kambe, N. Synthesis of imidazo and benzimidazo[2,1-a]-isoquinolines by rhodium-catalyzed intramolecular double C-H bond activation. *Org. Biomol. Chem.* **2013**, *11*, 2249–2253. [CrossRef]

49. Kozell, V.; Rahmani, F.; Piermatti, O.; Lanari, D.; Vaccaro, L. A stereoselective organic base-catalyzed protocol for hydroamination of alkynes under solvent-free conditions. *Mol. Catal.* **2018**, *455*, 188–191. [CrossRef]

50. Sheldrick, G.M. SHELXT-Integrated space-group and crystal-structure determination. *Acta Crystallogr. Sect. A Found. Adv.* **2015**, *71*, 3–8. [CrossRef]

51. Sheldrick, G.M. Crystal structure refinement with SHELXL. *Acta Crystallogr. Sect. C Struct. Chem.* **2015**, *71*, 3–8. [CrossRef] [PubMed]